RSC Advances

PAPER

View Article Online
View Journal | View Issue

Check for updates

Cite this: *RSC Adv.*, 2020, **10**, 41332

N,S-co-doped carbon dots for rapid acid test paper and bioimaging†

Juan Hou, [ab] Jing Qin,[a] Hongyu Pang,[a] Xu Gao, [a] Tiedong Sun [*a] and Bin Li[*ab]

Received 3rd September 2020
Accepted 26th October 2020

DOI: 10.1039/d0ra07550g

rsc.li/rsc-advances

Fluorescent N,S-CDs with a quantum yield of 37.8% were synthesized *via* a one-pot solvothermal method. Detailed characterizations on physical, chemical and optical properties have been investigated. N,S-CDs demonstrated remarkably quenched and enhanced fluorescence in acidic and basic media. Direct qualitative analysis in pH sensor and cell imaging were preliminarily studied.

Open Access Article. Published on 12 November 2020. Downloaded on 7/23/2025 11:24:24 AM.
This article is licensed under a Creative Commons Attribution-NonCommercial 3.0 Unported Licence.

Because of their excellent optical properties, low toxicity, photostability, high water solubility, easy synthesis and surface modification flexibility, fluorescent carbon dots (CDs) have attracted considerable attention for use in chemical and biological applications.[1–4] Recently, studies demonstrated CDs as one of the frontier fields in today's fluorescent materials science and have become more and more important due to their high resolution and fast response.[5–7]

pH value, expressed as the negative logarithm of H^+ concentration, plays an important role in environmental and biological processes like cell growth, diagenesis, and photosynthesis.[8–10] In recent years, fluorescent CDs-based nanosensors have been designed for pH detection in both environmental monitoring and *vivo*/*vitro* bioanalysis. For these fluorescent pH sensors, fluorescence intensity, emission wavelength and fluorescence lifetime are measured to specifically respond to different pH values. In our previous report, we prepared CDs from acetic acid using a microwave method and the CDs showed pH-sensitive FL feature.[11] Liu *et al.* reported a green anhydrous approach for the preparation of hydrophilic CDs with pH-sensitive property between 3 and 13.[12] Zhang *et al.* prepared a red/orange dual-emissive CDs for pH monitoring from 1.0 to 13.0.[13] Yu *et al.* reported a facile method for the synthesis of CDs with green fluorescence from phthalic acid and triethylenediamine hexahydrate. CDs was served as a pH nanosensor.[14] Compared to traditional organic dyes and semiconductor quantum dots, CDs-based sensors are superior in photo stability and low toxicity.[12,13] Most reported pH-responsive CDs exhibit a gradual change in fluorescence intensity by altering the pH value of the solution such that the pH can be detected. However, the fluorescence intensity often does not change much from one pH value to the neighbouring pH value. The testing process still needs to rely on fluorescence spectrometry for qualitative or quantitative analysis. Lack of visualization capability for directly performing qualitative analysis of the real sample under simple UV light by the naked eye is an obvious disadvantage.

Herein, we described a facile and efficient hydrothermal fabrication pathway for N,S co-doped CDs (abbreviated as N,S-CDs) with high quantum yield (~37.8%). The as-prepared N,S-CDs showed remarkably quenched and enhanced fluorescence in acidic and basic media. Their use in pH sensor and cell imaging were preliminarily studied.

N,S-co-doped CDs (N,S-CDs) were synthesized by hydrothermal treatment of citric acid and *N*-methyl thiourea at 180 °C for 7 h and purified by filter and dialysis (Scheme 1). The reaction yielded a yellow-brown solution with strong blue emissions. Full synthetic details and conditions optimization (starting material ratio, heating temperature and reaction time) have been listed in the ESI (Fig. S1†). Under the same optimal synthesis conditions, the reaction phenomena were consistent with various batches. The corresponding product yield could reach 69.1%.

The X-ray diffraction (XRD) pattern of the N,S-CDs displays a broad diffraction peak at around $2\theta = 24.8°$ due to the interlayer spacing of 0.34 nm, while the weak peak at nearly $2\theta = 41°$ represents the 0.21 nm interlayer spacing. The result is similar to that reported in other studies (Fig. S2†).[15,16] X-ray photoelectron spectroscopy (XPS) was conducted to confirm the chemical composition and surface state of N,S-CDs. Full scan XPS spectrum exhibits four typical peaks of C_{1s}, N_{1s}, O_{1s} and S_{2p} at 168, 285, 400 and 531 eV with atomic contents of 53.5%, 13.1%, 25.8% and 7.6%, respectively (Fig. S3†). The high-resolution spectra of C_{1s}, N_{1s}, O_{1s} and S_{2p} are shown in Fig S4.† C_{1s} spectrum shows three carbon states of C=O/C=N/C=S, C–C and C–O/C–S. Nitrogen exists in three forms of N–C_3, N–H and C–N–C. The O_{1s} spectrum can be resolved into two peaks attributed to C=O and C–O/C–N relevant groups. S_{2p} spectrum can be ascribed to the $2p_{3/2}$ and $2p_{1/2}$ positions of the

[a]*Department of Chemistry, Chemical Engineering and Resource Utilization, Northeast Forestry University, 26 Hexing Road, Harbin 150040, PR China*

[b]*Post-doctoral Mobile Research Station of Forestry Engineering, Northeast Forestry University, Harbin, 150040, PR China. E-mail: libinzh62@163.com; tiedongsun@nefu.edu.cn*

† Electronic supplementary information (ESI) available. See DOI: 10.1039/d0ra07550g

This journal is © The Royal Society of Chemistry 2020

Open Access Article. Published on 12 November 2020. Downloaded on 7/23/2025 11:24:24 AM.
This article is licensed under a Creative Commons Attribution-NonCommercial 3.0 Unported Licence.

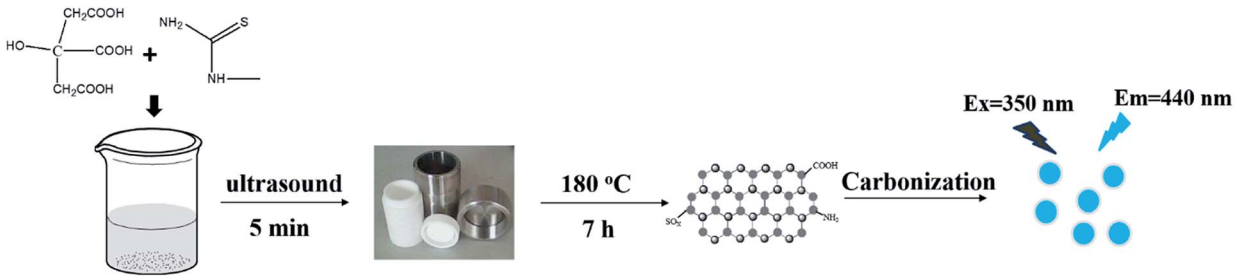

Scheme 1 The schematic of N,S-CDs preparation by hydrothermal pathway.

–C–S and –C–SO_x–. Therefore, the as-prepared N,S-CDs are rich in N and S heteroatoms.

The fluorescence spectra of N,S-CDs solutions (pH = 7.0) are shown in Fig. S5.† Increasing the excitation from 300 nm to 410 nm, the maximum emissions were located at 440 nm without shift, which demonstrated emission irrespective properties of the excitation wavelengths. However, CDs prepared from citric acid were observed as multi-color emissions (Fig. S6†). It is generally agreed that doped N and S may modify the surface states and lead to non-radiative transitions between the carbogenic core and surface state.[17,18] Using quinine sulfate in H_2SO_4 (0.1 mol L^{-1}) as the standard, the quantum yield of N,S-CDs was measured up to be 37.8%, which is 6.5 times higher than that of CDs derived from citric acid (5.8%). According to previous reports, doped N and S could introduce more passivated surface defects and enhance the fluorescent properties.[19,20] Long time storage, continuous UV exposure and ionic strength show little effects on the FL intensity of the N,S-CDs, suggesting its good time-, photo- and ionic-stability (Fig. S7†).

In the process of research, we found that the FL intensity of N,S-CDs possessed interesting pH response property. As shown in Fig. 1a and b, the N,S-CDs show strong emissions at 440 nm when excited at 350 nm. Tuning the pH value to the acidic region, the intensity suddenly reduces and emits almost no fluorescence. When the pH value is higher than 7.0, the intensity increased nearly doubled. After changing the pH value 7 times from 5.0 to 9.0 and then back to 5.0, the intensity does not change much from the original values under the same pH conditions, which indicates good pH reversible performance and response ability of N,S-CDs (Fig. 1c). Subsequently, the fluorescence intensity response to some relevant interfering species has been investigated. According to the results in Fig S8,† most metal ions and small bioactive molecules show little effect on the fluorescence, thus revealing good selectivity for pH monitoring based on the N,S-CDs.

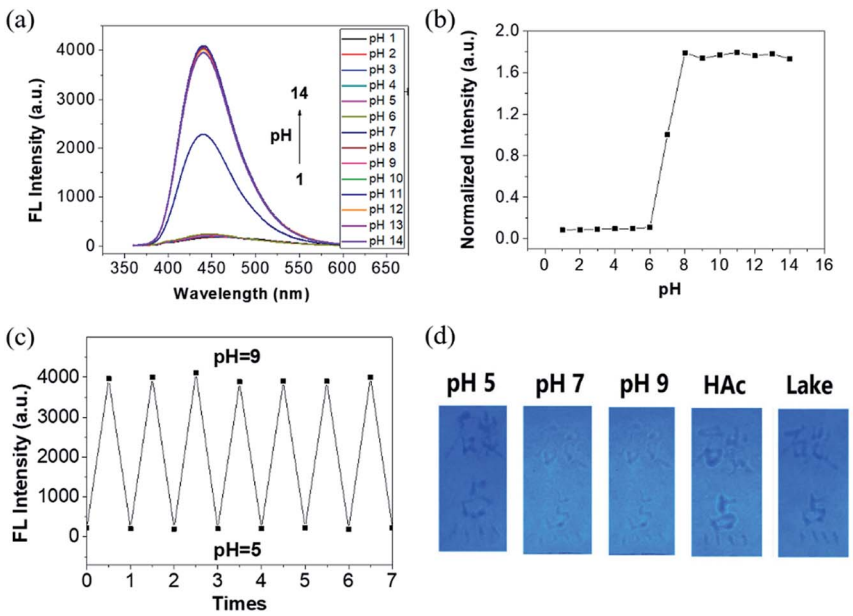

Fig. 1 (a) Fluorescence spectra (excited at 350 nm) of N,S-CDs in aqueous solution of different pH from 1 to 14; (b) change of normalized intensity with varying pH from 1 to 14; (c) the reversible pH-response of the FL behavior between pH 5.0 and 9.0 (excited at 350 nm); (d) optical photograph using the pH test paper prepared by N,S-CDs for the pH monitoring (left to right: pH = 5, 7, 9, 0.01 mol L^{-1} of HAc solution and real lake water, UV beam: 365 nm).

Open Access Article. Published on 12 November 2020. Downloaded on 7/23/2025 11:24:24 AM.
This article is licensed under a Creative Commons Attribution-NonCommercial 3.0 Unported Licence.

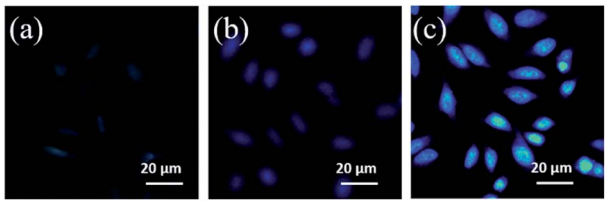

Fig. 2 Confocal fluorescence microscopy images of HeLa cells incubated with N,S-CDs (100 μg mL^{-1}) at 37 °C for 4 h in HEPES buffer with different pH of 5.0 (a), 7.0 (b) and 9.0 (c).

To collect insight on the size, morphology, surface chemistry and fluorescence change mechanism, N,S-CDs were characterized by TEM, UV and FTIR. Diluted N,S-CDs solutions (pH = 5, 7, 9) were dropped on carbon-coated copper grids for TEM measurement. The N,S-CDs solution of pH 5 showed a monodispersed spherical morphology with narrow size distribution between 1.5 and 4.0 nm (Fig. S9a†). When the pH value increased to 7, the particles began aggregation and formed a network-like structure (Fig. S9b†). In an alkaline environment (pH = 9), N,S-CDs are completely clustered together (Fig. S9c†). From the high-resolution TEM micrographs of a single dot, well-resolved lattice fringes can be observed with a typical lattice spacing of 0.21 nm, which can be ascribed to the (0 0 2) in-plane lattice of graphene (Fig. S9d†).[19] FTIR spectra shown in Fig. S10† demonstrate that some functional bonds of N,S-CDs in different pH environments such as C=O (1700 cm^{-1}), O–H (3450 cm^{-1}), C–O (1250 cm^{-1}), C–S (1129 cm^{-1}) and C=N/C=S (1397 cm^{-1}). In acidic condition, the typical peaks of N–H band at 3130 cm^{-1} and 1023 cm^{-1} are strong. With the increase in pH value, the intensities of N–H vibrations reduced, while new peaks at 2064 cm^{-1} and 1201 cm^{-1} emerged, which could be ascribed to the conjugated double bonds and C–N groups. The difference of FTIR spectra in various pH conditions may have resulted from the protonation–deprotonation of surface groups and solvent effects.[13] In acidic solution, the surface functional groups of N,S-CDs are protonated and positively charged. Additional electrophilic groups hinder the N,S-CDs from growing further. In neutral alkaline conditions, strong interactions between surface groups are enhanced because of polar–polar forces, van der Waal forces, H-bonding effects and electrostatic attraction, thereby increasing the conformational rigidity and affecting the morphology of N,S-CDs. The UV-vis absorption spectra of N,S-CDs with different pH values display strong absorption at high-energy region and a noticeable absorption band in a range of 380–450 nm, which is usually attributed to the π–π* transitions of C=C core and n–π* transitions of surface C=O/C=N groups (Fig. S11†).[21] Increasing the pH value from 6 to 8, the n–π* absorption band red shifts from 324 to 335 nm. At pH = 8, new absorption band appears at around 600 nm, mainly assigned to the n–π* transitions of conjugated C=S groups.[13] The fluorescence emissions of the as-prepared N,S-CDs was primarily generated by the n–π* transitions of the surface aromatic system containing C=O/C=N bands. A small shift of the absorption peak may be attributed to the change of surface functional groups. Combined with the above analysis, aggregation of the N,S-CDs leads to the n–π* absorption and FL intensity increasing based on the aggregation induced enhancement effect.[22–24]

Based on the good pH responsiveness and excellent photostability of the N,S-CDs, fluorescent test paper for visual sensing of pH have been constructed. Briefly, the filter paper was soaked into the N,S-CDs solutions for 30 s, air-dried for 10 min, and then cut into small pieces for pH detection. The test paper exhibited strong blue emission under a UV lamp of 365 nm. Solutions with different pH (pH = 5, 7, 9) were injected into a pen for painting patterns on the test paper (Fig. 1d). It can be seen by directly observing the color under UV light. Acid solution strongly quenched the fluorescence, and alkaline solution could enhance the emission. The quenched color by acid can be clearly distinguished with the naked eyes; therefore, the test paper could be used for direct acid recognition. Diluted acetic acid and real lake water samples were studied based on the prepared test papers with clear color reaction.

Intracellular pH (always around 7.4) is related to many physiological activities including cell growth and functions, which is of enormous importance in the fields of bio-medicine and molecular science.[9] In view of good fluorescence properties and excellent physiological dispersion of the N,S-CDs, their fluorescence imaging *in vitro* has been studied. Firstly, the cytotoxicity to living cells has been investigated using HeLa cells as a model system. As shown in Fig. S12,† the toxicity of the as-prepared N,S-CDs towards HeLa cells can be negligible even after 24 h. The cell viability is still higher than 80% at a concentration of about 600 μg mL^{-1}, which implies the biocompatibility of the N,S-CDs. To confirm the effectiveness of N,S-CDs in direct intracellular pH recognition, HeLa cells were co-cultured with N,S-CDs (100 μg mL^{-1}) at 37 °C for 4 h. Then, the cultured cells were treated in HEPES buffer with different pH (5.0, 7.0 and 9.0) and subjected to the confocal fluorescence imaging. As illustrated in Fig. 2, bright blue fluorescence signal of the HeLa cells could be observed after being incubated in HEPES buffer with pH = 7.0. When the pH is adjusted to 5.0, the images were quenched to nearly colorless. Moreover, when the pH increased to 9.0, the fluorescence was significantly increased. These observations illustrated a close correlation of fluorescence images intensity with the pH value in culture medium, which demonstrates that the N,S-CDs have potential applications in biological imaging and other associated biomedical applications.

Conclusions

In summary, we reported a facile, inexpensive preparation route for N,S-CDs *via* a one-pot hydrothermal method. The N,S-CDs show good fluorescence properties, low toxicity and high quantum yield. Due to the change of surface groups, the N,S-CDs demonstrate quenched emissions in acidic conditions and enhanced fluorescence in alkaline environment. The application of rapid acid test paper and intracellular bioimaging were preliminarily studied with good results. Hence, this work presents an adaptable naked-eye acid/base identification

 This journal is © The Royal Society of Chemistry 2020

Open Access Article. Published on 12 November 2020. Downloaded on 7/23/2025 11:24:24 AM.
This article is licensed under a Creative Commons Attribution-NonCommercial 3.0 Unported Licence.

protocol, which can be widely used in environmental and biomedical fields.

Conflicts of interest

There are no conflicts to declare.

Acknowledgements

We gratefully acknowledge the support from National Natural Science Foundation of China (NSFC, No. 21804017), China Postdoctoral Science Foundation (No. 2019M651242), and Heilongjiang Postdoctoral Science Fund (LBH-Z18009).

Notes and references

1 Z. Qian, X. Shan, L. Chai, J. Ma, J. Chen and H. Feng, *ACS Appl. Mater. Interfaces*, 2014, **6**, 6797.
2 H. Li, X. He, Z. Kang, H. Huang, Y. Liu, J. Liu, S. Lian, C. H. A. Tsang, X. Yang and S. Lee, *Angew. Chem., Int. Ed.*, 2010, **49**, 4430.
3 U. Baruah, N. Gogoi, G. Majumdar and D. Chowdhury, *Carbohydr. Polym.*, 2015, **117**, 377.
4 C. Wang, Z. Xu, H. Cheng, H. Lin, M. G. Humphrey and C. Zhang, *Carbon*, 2015, **82**, 87.
5 Y. Che, H. Pang, H. Li, L. Yang, X. Fu, S. Liu, L. Ding and J. Hou, *Talanta*, 2019, **196**, 442.
6 J. Li, S. Ma, X. Xiao and D. Zhao, *J. Nanomater.*, 2019, **2019**, 1.
7 Z. Wu, Z. Liu and Y. Yuan, *J. Mater. Chem. B*, 2017, **5**, 3794.
8 Z. Guo, Y. Jiao, F. Du, Y. Gao, W. Lu, S. Shuang, C. Dong and Y. Wang, *Talanta*, 2020, **216**, 120943.
9 J. Mandal, P. Ghorai, P. Brandaõ, K. Pal, P. Karmakar and A. Saha, *New J. Chem.*, 2018, **42**, 19818.
10 T. Zhang, S. Dong, F. Zhao, M. Deng, Y. Fu and C. Lü, *Sens. Actuators, B*, 2019, **298**, 126869.
11 J. Hou, L. Wang, P. Zhang, Y. Xu and L. Ding, *Chem. Commun.*, 2015, **51**, 17768.
12 X. X. Liu, C. L. Yang, B. Z. Zheng, J. Y. Dai, L. Yan, Z. G. Zhuang, J. Du, Y. Guo and D. Xiao, *Sens. Actuators, B*, 2018, **255**, 572.
13 M. Zhang, R. Su, J. Zhong, L. Fei, W. Cai, Q. Guan, W. Li, N. Li, Y. Chen, L. Cai and Q. Xu, *Nano Res.*, 2019, **12**, 815.
14 T. Yu, H. Wang, C. Guo, Y. Zhai, J. Yang and J. Yuan, *R. Soc. Open Sci.*, 2018, **5**, 180245.
15 H. Yang, Y. Liu, Z. Guo, B. Lei, J. Zhuang, X. Zhang, Z. Liu and C. Hu, *Nat. Commun.*, 2019, **10**, 1789.
16 L. Wang, Y. Bi, J. Hou, H. Li, Y. Xu, B. Wang, H. Ding and L. Ding, *Talanta*, 2016, **160**, 268.
17 Z. Guo, J. Luo, Z. Zhu, Z. Sun, X. Zhang, Z. Wu, F. Mo and A. Guan, *Dyes Pigm.*, 2020, **173**, 107952.
18 Y. Dong, H. Pang, H. B. Yang, C. Guo, J. Shao, Y. Chi, C. M. Li and T. Yu, *Angew. Chem. Int. Ed.*, 2013, **52**, 7800.
19 Z. Song, F. Quan, Y. Xu, M. Liu, L. Cui and J. Liu, *Carbon*, 2016, **104**, 169.
20 H. Ding, J. S. Wei and H. M. Xiong, *Nanoscale*, 2014, **6**, 13817.
21 D. Wang, Z. Wang, Q. Zhan, Y. Pu, J. Wang, N. R. Foster and L. Dai, *Engineering-PRC.*, 2017, **3**, 402.
22 W. Lv, M. Lin, R. Li, Q. Zhang, H. Liu, J. Wang and C. Huang, *Chin. Chem. Lett.*, 2019, **30**, 1410.
23 Y. Xu, H. Li, B. Wang, H. Liu, L. Zhao, T. Zhou, M. Liu, N. Huang, Y. Li, L. Ding and Y. Chen, *Microchim. Acta*, 2018, **185**, 1.
24 C. Wang, K. Jiang, Z. Xu, H. Lin and C. Zhang, *Inorg. Chem. Front.*, 2016, **3**, 514.